RSC Advances

COMMUNICATION

View Article Online
View Journal | View Issue

Thermochemical analysis on the growth of $NiAl_2O_4$ rods†

Cite this: *RSC Adv.*, 2014, **4**, 1159

Sang Sub Kim,[a] Gun-Joo Sun,[a] Hyoun Woo Kim,*[b] Yong Jung Kwon[b] and Ping Wu*[c]

Received 25th June 2013
Accepted 14th November 2013

DOI: 10.1039/c3ra43196g

www.rsc.org/advances

We have succeeded in growing cubic submicron-sized $NiAl_2O_4$ rods on sapphire substrates by means of heating a mixture of NiO and graphite powders. At 1600 °C, $NiAl_2O_4$ rods terminated by SiO_x-containing nanoparticles were grown on the sapphire substrates. In contrast, NiO rods grew randomly at 1500 °C. We elucidated the growth steps of cubic $NiAl_2O_4$ submicron-sized rods on the basis of a thermochemical approach, revealing the critical role of liquid silica that blocks the continuous loss of Ni to the vapor phase for the successful growth of $NiAl_2O_4$ rods.

Introduction

Nickel aluminate ($NiAl_2O_4$) is a mixed-cation oxide with normal spinel structure in which Al occupies the octahedral and Ni the tetrahedral sites. Industrial applications of this material are mainly ascribed to its stable structure at high temperatures and its catalytic features,[1] combined with a high surface area. In addition, $NiAl_2O_4$ is a promising candidate for use as anode material in aluminum electrolysis because of a unique combination of electrical conductivity and chemical diffusivity.[2] It can also be used as core insulating material in power fusion reactors due to its radiation stability. Furthermore, it has potential for application as a refractory material in the ceramics industry due to its low density (3.58 g cm^{-3}) and its stability in harsh environments.[3] Also, it has been used as a humidity sensor with interesting results in terms of sensitivity, stability, and response time.[4–6] Since the high surface area of $NiAl_2O_4$ is critical for industrial applications, including catalysis, the fabrication of $NiAl_2O_4$ nanoparticles has been intensively studied by means of a variety of methods, including sol–gel[7] and sonochemical synthesis.[8] In addition, nanoscale $NiAl_2O_4$ has been formed during NiAl (111) oxidation.[9]

One-dimensional (1D) structures have attracted great attention due to their peculiar physical properties and potential applications, thus focusing on investigations related to mesoscopic physics and the fabrication of nano-devices, respectively. Furthermore, the development of methods for synthesizing a wide variety of 1D structures made from novel materials has become increasingly important. Although 1D structures provide peculiar and interesting physical properties, to the best of our knowledge, no attempt has been reported on the preparation of 1D nano- or microrods of $NiAl_2O_4$. Their shape with a large surface-to-volume ratio indicates that they will exhibit useful physical and chemical properties. Accordingly, a variety of applications, including in electrodes, sensors, and insulators, is expected.

In the present paper, we report on the fabrication of 1D structures of $NiAl_2O_4$ at the submicron scale. This has been accomplished by heating a mixture of NiO and graphite powders. On the basis of a thermochemical analysis, we propose the growth mechanism of $NiAl_2O_4$. In particular, we revealed that liquid silica played a critical role in blocking the continuous loss of Ni to the vapor phase. Detailed experimental procedures are described in ESI.† Previously, Sivakumar *et al.* synthesized $NiFe_2O_4$ nanorods by a polymer-assisted co-precipitation method using polyethylene oxide (PEO) as a capping and a polymer structure directing reagent.[10] Herein, they revealed that the concentration of PEO/$NiFe_2O_4$ composite is controlling the formation, size, and shape of the nanorods. Also, Nanko *et al.* prepared $NiAl_2O_4$ nanorod arrays by the pack cementation process, in which Ni matrix is oxidized together with Al_2O_3 rods.[11] In the present work, the well-known vapor–liquid–solid (VLS) mechanism was employed to obtain the 1D $NiAl_2O_4$ rods. While most previous VLS studies are associated with metal catalyst tips which should be removed for applications,[12,13] we have produced the SiO_x particles at the tips of the rods, which can be useful in a combination scheme.

[a]*Department of Materials Science and Engineering, Inha University, Incheon 402-751, Republic of Korea*

[b]*Division of Materials Science and Engineering, Hanyang University, Seoul 133-791, Republic of Korea. E-mail: hyounwoo@hanyang.ac.kr*

[c]*Entropic Interface Group, Singapore University of Technology & Design, Singapore 138682, Singapore. E-mail: wuping@sutd.edu.sg*

† Electronic supplementary information (ESI) available. See DOI: 10.1039/c3ra43196g

Results and discussion

XRD patterns are included in ESI (Fig. S2†) The diffraction peaks in XRD pattern of the product grown at 1500 °C can be indexed on the basis of two phases, namely, cubic NiO with lattice constants comparable to the reference values reported in the JCPDS 47-1049 card and cubic $NiAl_2O_4$ with normal spinel structure with lattice constants $a = 8.048$ Å (JCPDS: 10-0339). On the other hand, the product grown at 1600 °C is mainly comprised of cubic $NiAl_2O_4$ with a trace amount of the cubic NiO phase. SEM and TEM analyses were carried out for the rods grown at 1500 °C (Fig. S3†). Both the TEM image and the SAED pattern indicate that the rods are mainly comprised of the NiO phase (Fig. S3†), whereas the XRD investigation reveals the existence of a considerable amount of $NiAl_2O_4$ (Fig. S2†). Further plan-view SEM observations exhibit the presence of film-like or cluster-like products, which are indicated by dotted areas in Fig. S4.† Therefore, it is reasonable to conclude that rods of NiO grew on sapphire (0001) substrates with a buffer layer of $NiAl_2O_4$ at 1500 °C.

Fig. 1(a and b) shows SEM images of the product grown at 1600 °C. Fig. 1(a) exhibits that the 1D rods were grown with various angles on the substrate. The enlarged SEM image indicates that the rods have spherical nanoparticles at their tips (Fig. 1(b)). The low-magnification TEM image confirms that rounded nanoparticles are attached to the tip. Fig. 1(c–g) exhibits the elemental maps of Ni, Al, O, and Si. It is observed that the region in which the rods were grown is comprised of the elements Ni, Al, and O. The elements Si and O are preferentially located in the tip region. Fig. 1(h) and (i) show a SAED pattern and a lattice-resolved TEM image, respectively, from a surface region of the rods grown at 1600 °C. The SAED pattern was recorded perpendicular to the rod axis, which is parallel to the $[01\bar{1}]$ zone axis of cubic $NiAl_2O_4$. The well-defined SAED pattern clearly shows diffraction spots representing $(\bar{1}11)$, (111), and (200) lattice planes of the cubic $NiAl_2O_4$ structure. On the basis of the lattice-resolved TEM image, the interlayer distances were determined to be about 0.20 nm and 0.46 nm, corresponding to the spacings d_{200} and d_{110} of the cubic $NiAl_2O_4$ lattice.

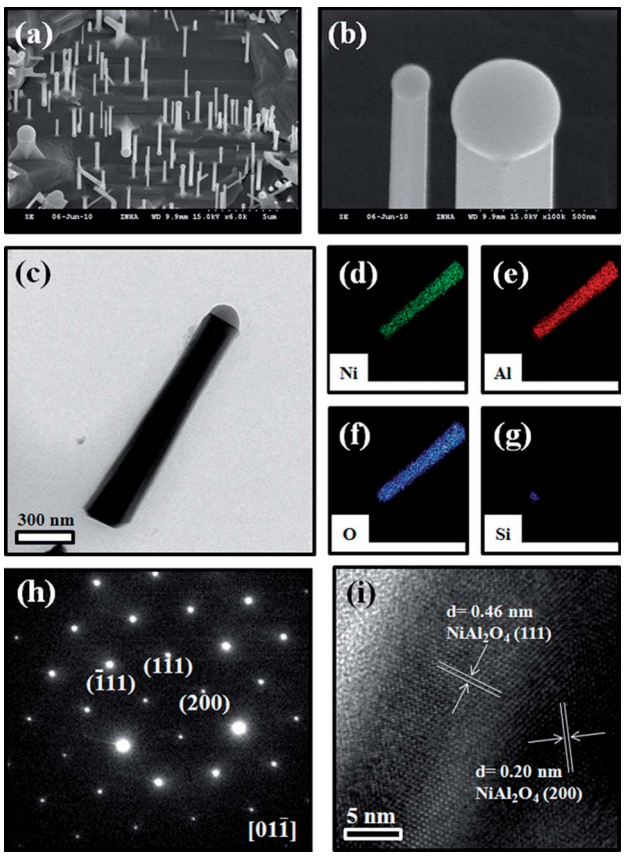

Fig. 1 (a and b) SEM image and (c) low-magnification TEM image of 1600 °C-grown rods. EDX elemental maps of (d) Ni, (e) Al, (f) O, and (g) Si elements. (h) SAED pattern and (i) lattice-resolved TEM image of 1600 °C-grown rods.

Based on the current investigations (XRD, SEM, and TEM) and literature reports,[14–18] we performed an additional thermochemical analysis aiming at a better understanding about the growth mechanism of the 1D $NiAl_2O_4$ rods. De Roos *et al.*[14] proposed that the nucleation of $NiAl_2O_4$ at the NiO–Al_2O_3 interface starts with Al^{3+} ions (penetrating along the grain boundaries of NiO) followed by counter-diffusion of Ni^{2+} ions, which is expected since Al^{3+} is smaller in size than Ni^{2+}. The essential role of oxygen diffusion under various growth conditions of $NiAl_2O_4$ was studied by Zhong *et al.*[15] and was further confirmed by Kotula *et al.*[16] In addition, Loginova *et al.*[17] pointed out that repeated cycles of oxygen exposure (a dynamic process) lead to nucleation of $NiAl_2O_4$. Recently, Chen *et al.*[18] synthesized carbon nanofibers from CO_2 by using a Ni–Al_2O_3 catalyst. It seems that the introduction of carbon into the NiO–Al_2O_3 system may lead to different products ranging from carbon nanofibers[14] to spinel nanorods (in this work), depending on the thermochemical constrains imposed on the system. Therefore, it is important to understand the unique thermodynamic behavior of the C–SiO_2–NiO–Al_2O_3 system. There are three phases involved in the spinel synthesis; gas (air and Ar), liquid (silica) and solid (C, SiO_2, NiO, Al_2O_3, and $NiAl_2O_4$) material. We used a commercial thermochemistry simulation software, FactSage, for the following synthesis analysis performed at 1600 °C (amounts are given in moles):

I. Reactions between carbon and each of the three binary oxides

$$C + SiO_2 = 0.66SiO_2 + 0.33SiC + 0.69\ \text{gas (97.4\% CO, 2.5\% SiO)} \quad (1)$$

1/3 of solid SiO_2 is reduced to 1/3 of solid SiC and a minor amount of SiO in the gas phase. As shown below, the formation of minor quantity of SiO in the gas phase is critical to the synthesis process.

$$C + Al_2O_3 = C + Al_2O_3 \quad (2)$$

No chemical reaction is expected between C and Al_2O_3.

$$C + NiO = Ni + \text{gas (100\% CO)} \quad (3)$$

NiO is reduced to Ni and the concomitantly formed gas phase consists of 100% CO. In other words, Ni is easily removed from the solid to the gas phase.

II. The partition of metals (Ni, Al, and Si) between the gas and the liquid (silica) phase determined by assuming that $NiAl_2O_4$ is the only solid phase, which is reasonable considering the trace amount of the cubic NiO phase.

$$C + SiO_2 = 0.13SiO_2\ (liquid) + 1.78\ gas\ (54\%\ CO, 44\%\ SiO, 2\%\ SiC) \quad (4)$$

We see that a sufficient amount of SiO is built up in the gas phase to supply Si for the formation of liquid SiO_2.

$$C + NiO = 2\ gas\ (50\%\ Ni, 50\%\ CO) \quad (5)$$

No liquid phase is formed. All Ni^{2+} ions of NiO have been reduced to Ni° in the gas phase. Without additional protection, all Ni may be transferred to the gas phase prior to interacting with Al to form the spinel compound.

III. Reactions in the system of gas, liquid (silica slag), and solid (spinel, SiO_2)

$$C + Al_2O_3 + NiO + SiO_2 = 2.00\ gas\ (47\%\ Ni, 50\%\ CO, 3\%\ SiO) + 1.78\ liquid\ (52.9\%\ SiO_2, 44.8\%\ Al_2O_3, 2.3\%\ NiO) + 0.156\ spinel. \quad (6)$$

The liquid phase is formed with a low solubility of NiO (47% in gas and 2.3% in liquid), therefore, we may use the liquid phase to block the loss of Ni from NiO to the gas phase. Here are two evidences. First, liquid silica is formed at the top of the $NiAl_2O_4$. In Fig. 1(g), Si element was observed mainly at the top of the rod. Based on the thermodynamics calculation shown in eqn (6), 94% and 6% of Si located at the top are in the liquid and gas phases, respectively, at 1600 °C. Therefore, at the top of the rod, this enriched Si is mainly in the liquid form of SiO_2 at 1600 °C, which will separate the solid rod from the gas phase. Second, Ni has much lower solubility in liquid SiO_2 than in gas SiO: based on the thermodynamics calculation shown in eqn (6), 94%, 4%, and 2% of all Ni are in the gas, liquid and solid phases, respectively, at 1600 °C. Therefore, less Ni will be lost into liquid SiO_2 (4%) than into gas SiO (94%). The top liquid SiO_2 layer cuts off the loss of Ni to the gas phase by blocking the direct contact of solid to gas phase. This will ensure sufficient supply of Ni for the formation of $NiAl_2O_4$. Based on the above thermochemical analysis, it is clear that the formation of the liquid silica phase is a critical step for the successful synthesis of $NiAl_2O_4$.

There are two well-accepted mechanisms for the growth of 1D nanostructures: the VLS and the vapor–solid (VS) mechanism. In the present growth process at 1600 °C, the existence of particles at the ends of the rods suggests that the growth mechanism is associated with the VLS process. The growth of $NiAl_2O_4$ rods at 1600 °C with nanoparticles attached to the end of the rods can be divided into several steps by taking the above thermochemical analysis into account. In the first step, a mixture of NiO and graphite powders was heated and evaporated according to eqn (5). We surmise that Si atoms within the liquid droplets originate from the chamber ambience, as shown by eqn (4). More detailed, we believe that the silicon contained in the liquid droplets originates from the surface of the quartz tube and/or from the silica component of the alumina boat.

At a high temperature of 1600 °C, some Si atoms will evaporate from the quartz surface. This can be corroborated from the fact that the melting point of quartz is in the range of 1600–1800 °C (*i.e.*, 1670 °C (β-tridymite); 1713 °C (β-cristobalite)). Also, it is possible that oxidation of Si occurs, consequently resulting in the formation of SiO gas[19] (as indicated by eqn (4)). The thus formed volatile Si suboxide vapor could preferentially decompose at the surface of a liquid droplet. Ultimately, Si/Ni/Al/O liquid droplets are formed on top of the substrate (Fig. 2). From the $NiAl_2O_4$–SiO_2 phase diagram shown in the ESI (Fig. S5†),[20] we suppose that there exists an eutectic-like reaction between $NiAl_2O_4$ and SiO_2 at around 1495.5 °C. Accordingly, starting from Si/Ni/Al/O liquid droplets with a sufficient amount of Ni and Al, the liquid droplets become supersaturated when the temperature decreases and the relative amount of Ni and Al increases, as shown by eqn (6). In the second step, as droplets or nanoparticles acting as nucleation sites become supersaturated, such that the concentration of Ni and Al in the alloy droplets or nanoparticles exceeds the saturation threshold, the growth of $NiAl_2O_4$ rods is initiated as a result from the reaction between Ni, Al, and O (Fig. 2). Accordingly, the remaining alloy droplets will be comprised of SiO_2. This is in agreement with the EDX results (Fig. 1), according to which the elements Si and O are preferentially located within the tip region.

On the other hand, during the growth process at 1500 °C, which is only 4.5 °C higher than the eutectic-like reaction presented in Fig. S5,† rods with particle-free ends were preferentially formed. It is likely that the liquid silica phase is not formed at 1500 °C, even though it is higher than 1495.5 °C, due to chemical kinetics constraints. Therefore, instead of a single liquid phase covering the top of the rods and preventing depletion of Ni to the gas phase (eqn (5)), a mixture of three solid phases (NiO, spinel, and cristobalite) may be formed, which is much less effective in insulating the top of the rods from the gas phase. This proposed mechanism is supported by the XRD and TEM data that suggest that the main constituent of the rods was cubic NiO, rather than cubic $NiAl_2O_4$. By increasing the temperature from 1500 to 1600 °C, the amount of the liquid silica phase will increase in a continuous manner. This tendency will be associated with the following two phenomena. First, with increasing the temperature, the amount

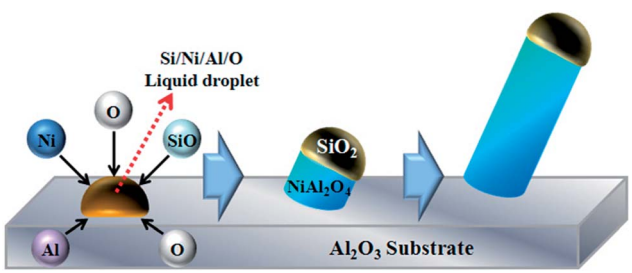

Fig. 2 Schematic illustration of the growth process at a substrate temperature of 1600 °C.

of vapour Si atoms will be increased. Second, at a higher temperature, it will be easier to form Si/Ni/Al/O liquid on top of the substrate. Since the volatile Si suboxide vapor decomposes at the surface of a liquid droplet, the abundance of liquid droplet at a higher temperature will contribute to the increase of the amount of the liquid silica phase. In order to reveal the detailed structure/morphology of the products at temperatures between 1500 and 1600 °C, further systematic study is necessary.

A room-temperature PL spectrum of the rods grown at 1600 °C is shown in the ESI (Fig. S6†). To reveal the origin of these bands, we have compared the PL spectra of the rods grown at 1600 °C and at 1500 °C (Fig. S6† and its inset). While the peak at 2.4 eV can be mainly attributed to the NiO phase, we suggest that the peak at 2.7 eV arises from the SiO_x phase of the rod tips.

Conclusions

We have synthesized submicron-sized rods of $NiAl_2O_4$ at a temperature of 1600 °C on sapphire substrates. While the products synthesized at 1600 °C are mainly comprised of submicron-sized rods of $NiAl_2O_4$ with SiO_x particles at the ends of the rods, the product grown at 1500 °C is formed by particle-free NiO submicron rods. Accordingly, it is revealed that the growth at 1600 °C is mainly controlled by a VLS mechanism in which $NiAl_2O_4$ rods are grown with remnant SiO_x becoming tip particles. By thermochemical analysis, we revealed that diffusion kinetics plays a key role in the formation of the $NiAl_2O_4$ phase. The formation of a liquid phase on top of the rod may block the continuous depletion of Ni^{2+} into the gas phase and provide a steady supply of Ni to match the fast diffusion of Al^{3+} ions.

Acknowledgements

Dr Ping Wu's research is partially sponsored by the SUTD-ZJU grant (SUTD-ZJU/RES/01/2012) on chemical sensing and by Singapore MOE Tier 2 grant (MOE 2012-T2-1-097) on interface transport.

Notes and references

1 A. Al-Ubaid and E. E. Wolf, *Appl. Catal.*, 1988, **40**, 73.
2 J. Shin, A. Goyal, K. More and S.-H. Wee, *J. Cryst. Growth*, 2008, **311**, 210.
3 A. Laobuthee, S. Wongkasemjit, E. Traversa and R. M. Laine, *J. Eur. Ceram. Soc.*, 2000, **20**, 91.
4 G. Gusmano, G. Montesperelli, E. Traversa and G. Mattogno, *J. Am. Ceram. Soc.*, 1993, **76**, 743.
5 T. Seiyama, N. Yamazoe and H. Arai, *Sens. Actuators, B*, 1983, **4**, 85.
6 Y. Shimizu, H. Arai and T. Seiyama, *Sens. Actuators, B*, 1985, **7**, 11.
7 H. Cui, M. Zayat and D. Levy, *J. Non-Cryst. Solids*, 2005, **351**, 2102.
8 P. Jeevanandam, Y. Koltypin and A. Gedanken, *Mater. Sci. Eng., B*, 2002, **90**, 125.
9 E. Loginova, F. Cosandey and T. E. Madey, *Surf. Sci. Lett.*, 2007, **601**, L11–L14.
10 P. Sivakumar, R. Ramesh, A. Ramanand, S. Ponnusamy and C. Muthamizhchelvan, *J. Appl. Phys.*, 2013, **563**, 6.
11 M. Nanko, D. T. M. Do and T. Ishizaki, *Curr. Appl. Phys.*, 2012, **12**, S184.
12 R. S. Wagner and W. C. Ellis, *Appl. Phys. Lett.*, 1964, **4**, 89.
13 A. M. Morales and C. M. Lieber, *Science*, 1998, **279**, 208.
14 G. De Roos, J. M. Fluit, R. P. Velthuizen, J. H. W. De Wit and J. W. Geus, *Surf. Interface Anal.*, 1983, **5**, 119.
15 Q. Zhong and F. S. Ohuchi, *J. Vac. Sci. Technol., A*, 1990, **8**, 2107.
16 P. G. Kotula and C. B. Carter, *J. Am. Ceram. Soc.*, 1998, **81**, 2869.
17 E. Longinova, F. Cosandey and T. E. Madey, *Surf. Sci.*, 2007, **601**, L11.
18 C. S. Chen, J. H. You and C. C. Lin, *J. Phys. Chem. C*, 2011, **115**, 1464.
19 D. Starodub, E. P. Gusev, E. Garfunkel and T. Gustafsson, *Surf. Rev. Lett.*, 1999, **6**, 45.
20 B. Phillips, J. J. Hutta and I. Warshaw, *J. Am. Ceram. Soc.*, 1963, **46**, 579.

